GLUEBALLS IN THE REACTION $\pi^- p \rightarrow \phi\phi n$ †

S.J. Lindenbaum

Brookhaven National Laboratory, Upton, New York 11973

and

City College of New York, New York, New York 10031

Invited Lecture at the XVIII Rencontre De Moriond Elementary Particle Physics Meeting, Savoie, France, January 23-29, 1983.

† This research was supported by the U.S. Department of Energy under Contract Nos. DE-AC02-76CH00016 (BNL) and DE-AC02-79ER10550A (CCNY).

GLUEBALLS IN THE REACTION $\pi^- p \rightarrow \phi\phi n$ †

S.J. Lindenbaum
Brookhaven National Laboratory, Upton, New York 11973
and
City College of New York, New York, New York 10031

Abstract

The BNL/CCNY group has observed and performed a partial wave analysis on 1203 (22 GeV) $\pi^- p \rightarrow \phi\phi n$ events. The OZI suppression has been found to be almost completely broken down. The $\phi\phi$ spectrum is found to be composed almost entirely of two new resonances, the $g_T(2160)$ and the $g_T(2320)$ with $I^G J^{PC} = 0^+2^{++}$. For g_T (2160), $M = 2.16 \pm 0.05$ GeV, and $\Gamma = 0.31 \pm 0.07$ GeV. For $g_T(2320)$, $M = 2.32 \pm 0.04$, and $\Gamma = 0.22 \pm 0.07$. Assuming 1) QCD is correct, and 2) the OZI rule is universal for weakly coupled glue in disconnected Zweig diagrams due to the creation or annihilation of new types of quarks; it is concluded that one or two primary glueballs with the above quantum numbers are responsible for the above observed states.

Introduction

In a pure Yang-Mills theory[1] where $SU(3)_c$ has local gauge symmetry, and color is confined, all hadrons would be glueballs[2] (i.e. multi-gluon resonances). This is due to the self-coupling of the gluons which becomes stronger with decreasing energy (i.e. asymptotic freedom).

However experimentally we find that the hadronic sector is dominated by $q\bar{q}$ and qqq built states. There were a number of glueball candidates and extensive discussion of them.[3-20]

† This research was supported by the U.S. Department of Energy under Contract Nos. DE-AC02-76CH00016 (BNL) and DE-AC02-79ER10550A (CCNY).

Thus establishing glueballs is crucial to any theory which uses $SU(3)_c$ such as QCD, Grand Unification and Partial Unification. It has been the author's opinion for some time[5,6] that if glueballs are not established, QCD is in serious trouble. On the other hand, the explicit establishment of glueballs would indeed be a great triumph for QCD.

How Do You Find Glueballs?

From prior experimental observation it is clear that if glueballs exist, they are masked in the vast collection of quark-built meson nonets, existing in the mass range where one would expect to find them (≈ 1-3 GeV).

1. Pattern Recognition of a Decuplet

One looks for a nonet with an extra singlet, a glueball with the same quantum numbers. If it is near enough to the singlets in the nonet it will mix with them. Nonet + glueball + decuplet, with characteristic mixing and splitting (and have other special characteristics of glueballs). Calculations have shown that the ideal mixing observed in a great deal of nonets would be affected in these decuplets, and pattern recognition would have to be used.[19,20] A glueball candidate of this type is the BNL/CCNY $J^{PC} = 0^{++}$ $g_s(1240)$.[15] This would make a new 0^{++} multiplet with apparently the right characteristics: Of course one must realize that there are many other possible explanations for these states.*

2. Look in a Channel Enriched in Gluons

Glueball candidates of this type are the SLAC $J^{PC} = 0^{-+}$, iota(1440), which could be the tenth member of a ground state 0^{-+} decuplet,** and the SLAC θ (1640). On course one should realize that there are many other possible explanations for these states. Secondly, the following speaker[21] will discuss the iota and the θ followed by three theoretical talks on the subject.[22-24]

3. An OZI Suppressed Channel with a Variable Mass

In an OZI suppressed channel with variable mass, glueballs with the right quantum numbers should break down the OZI suppression in the mass region where they exist and dominate the channel. Thus the OZI suppression can act as a filter for letting glueballs pass while suppressing other states. Furthermore, the breakdown of the OZI suppression can serve as a clear signal that one or more glueballs are present in the mass region. According to present concepts in QCD, the OZI suppression is due to the fact that two or more hard gluons are needed to

---

* One could, for example, inadvertently mix states from the basic nonet with those of a radial excitation.

** The SLAC iota(1440) is thought to be in a channel where glueballs are enhanced since it is found in J/ψ radiative decay.

bridge the gap in an OZI suppressed disconnected or hairpin diagram involving new types of quarks. The early onset of asymptotic freedom leads to a relatively weak coupling constant for these gluons, which then causes the OZI suppression. However, if the glue in the intermediate state resonates to form a glueball, the effective coupling constant (as in all resonance phenomena) must become strong, and the OZI suppression should disappear in the mass range of the glueball. This should allow hadronic states with the glueball quantum numbers to form with essentially no OZI suppression. The author has made this argument previously.[5,6,14,15] Thus the OZI suppression essentially is a filter which lets glueballs pass and suppresses other states.

<u>The $\pi^-p \to \phi\phi n$ (OZI Forbidden Channel)</u>

My lecture will be concerned with this channel since the latest detailed results have been obtained in it.

The BNL/CCNY collaboration had shown in 1977-78 that in the OZI forbidden[25] (or suppressed) reaction $\pi^-p \to \phi\phi n$ at an incident pion energy of 22.6 GeV, that the OZI suppression was essentially absent.[4] This was quantitatively demonstrated, and interpreted by the author as evidence for glueballs in the $\phi\phi$ system.[5,6] However, the initial 100, and eventual 170 events obtained did not allow a viable partial wave analysis to explicitly identify the glueball candidates quantum numbers, mass, width, etc. The $\phi\phi$ mass spectrum observed in other later low statistics measurements were consistent with our results.[26]

The BNL MPS (Multiparticle Spectrometer) was redesigned with a novel, high speed drift chamber system replacing the spark chambers[27] in order to obtain > an order of magnitude more data. In a run with the new MPS II and 22 GeV incident π^- beam, BNL/CCNY obtained 1203 $\pi^-p \to \phi\phi n$ events in which the visible cross section is only ≈ 6 nanobarns.

A partial wave analysis of this data[15,29] yields at the very least, two explicit strong glueball candidates in the $\phi\phi$ system with all quantum numbers, mass and width determined. As will be discussed later if QCD is correct and the OZI rule universal for disconnected OZI suppressed diagrams, one or two primary glueballs have resulted in these states.

The basic reaction measured is given by the OZI allowed reaction (Fig. 1a) $\pi^-p \to K^+K^-K^+K^-n$. In QCD[28] one considers these OZI allowed reactions proceed by a continuous series of exchanges of single and perhaps some low energy multiple gluons which have relatively strong effective coupling constants and thus are strong interactions. The poorly understood hadronization process is thought to a large extent to occur near the outer regions of the confinement region with unsuppressed cross sections.

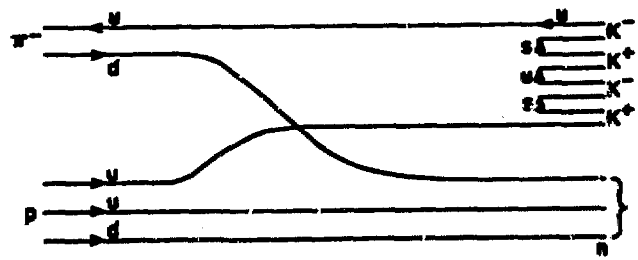

Figure 1a: The quark line diagram for the reaction $\pi^-p \to K^+K^-K^+K^-n$, which is connected and OZI allowed.

If a ϕ replaces one K^+K^- pair we have the reaction $\pi^-p \to \phi K^+K^-n$ (see Fig. 1b) which is still a connected diagram and OZI allowed.

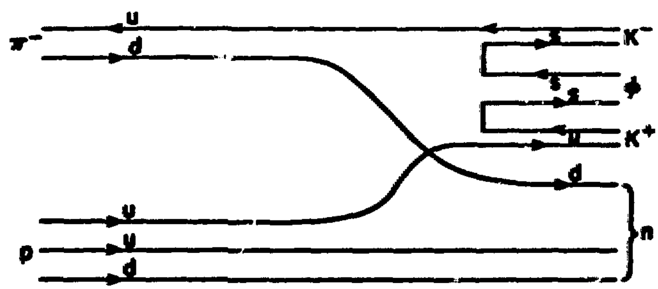

Figure 1b: The quark line diagram for the reaction $\pi^-p \to \phi K^+K^-n$, which is connected and OZI allowed.

However, if both K^+K^- pairs form ϕ's, we have a disconnected (double hairpin) diagram which is OZI forbidden. Hence $\pi^-p \to \phi\phi n$ in Fig. 1c is an OZI forbidden diagram, and should exhibit the OZI suppression.

This was clearly shown for $\pi^-p \to \phi n$, where the OZI suppression factor is ≈ 100.[30] Typically:

$$\frac{\sigma(\pi^-p) \to \omega n}{\sigma(\pi^-p) \to \phi n} \approx 100$$

also exhibiting the OZI suppression factor.

Another OZI allowed process is $K^-p \to \phi\Lambda$. The ratio

$$\frac{\sigma(K^-p) \to \phi\Lambda}{\sigma(\pi^-p) \to \phi n} \approx 60$$

also shows the typical OZI suppression.[31]

The decay matrix element squared of the OZI allowed process, $\phi \to K^+K^-$, is ≈ 100 times that for $\phi \to \rho^+\pi^-$ which is OZI suppressed.[25a] Hence in both the

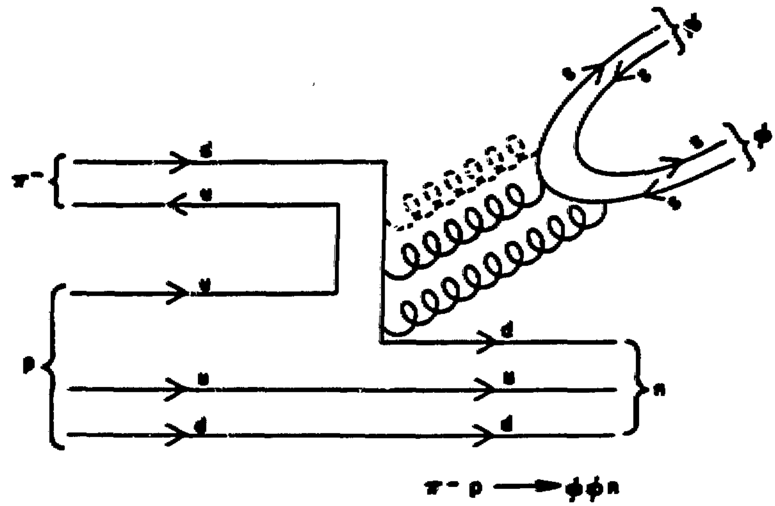

Figure 1c: The quark line diagram for the reation $\pi^- p \to \phi\phi n$ which is disconnected (i.e. a double hairpin diagram) and is OZI forbidden. Two or three gluons are shown connecting the disconnected parts of the diagram depending upon the quantum numbers of the $\phi\phi$ system.

production and decay, a single ϕ hairpin (disconnected diagram, see Fig. 2), corresponds to an OZI suppression factor ≈ 100.

One may ask is it as legitimate to consider $\pi^- p \to \phi\phi n$ also as a disconnected diagram subject to the OZI suppression. Each of the two ϕ's is an almost pure $s\bar{s}$ meson system. If you look at Fig. 1c from right to left you have two $s\bar{s}$ states disconnected from the π^-, p and n part of the diagram which is connected, and contains only u and d quarks. This is basically a disconnected diagram just like the OZI suppressed single ϕ production case.

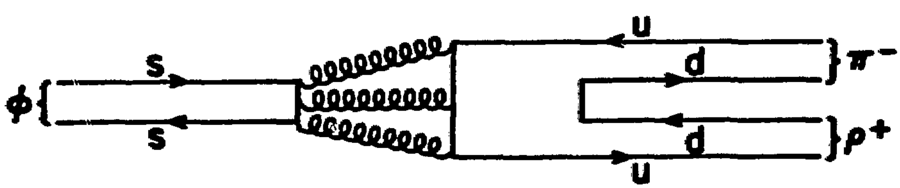

Figure 2a: The quark line diagram for the reaction $\phi \to \rho^+\pi^-$ which is disconnected and OZI forbidden.

An experimental example where a disconnected diagram formed by two particles in the final state composed of new types of quarks and their antiquarks leads to OZI suppression[32] is shown in Fig. 2c (left half):

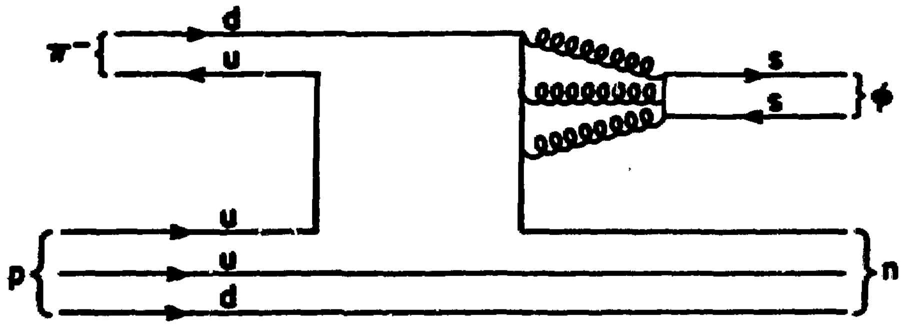

Figure 2b: The quark line diagram for the reaction $\pi^- p \rightarrow \phi n$ which is a disconnected and OZI forbidden.

$$\psi(3685) \rightarrow J/\psi\ \pi^+\pi^-\ (33 \pm 2)\%, \text{ or } J/\psi\ \pi^0\pi^0\ (17 \pm 2)\%.$$

The full width of the $\psi(3685)$ is only 0.215 MeV, clearly showing the strong OZI suppression corresponding to the fact that that initial state contains $c\bar{c}$ quarks only, whereas the final state still contains the $c\bar{c}$ quarks but the diagram becomes disconnected when u and d quarks and their antiquarks (to form the two pions) are included in the final state. Only the decay mode involving $\pi^+\pi^-$ is shown, but one should remember that there is an additional decay mode involving π^0 with about half the rate. If this process were OZI allowed, the $\psi(3685)$ would be very much wider. These Zweig diagrams have two separate disconnections, one containing a double hairpin and the other having the more commonly observed single hairpin, and the OZI rule works beautifully at each disconnection.

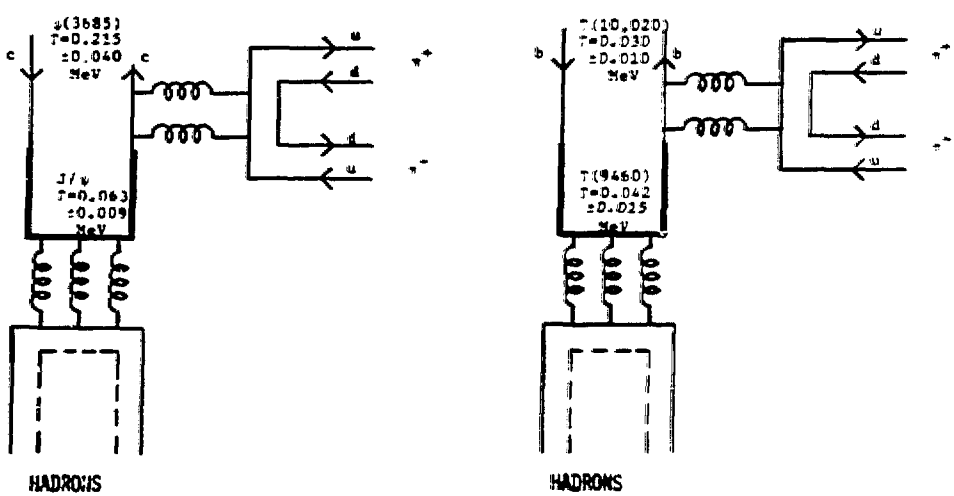

Figure 2c

The right half of Fig. 2c shows a similar reaction in the Υ system where the Υ(10,020) → Υ(9460) ππ (30 ± 6)% of the time. This case is an even more impressive example since for the Υ(10,020), Γ = 0.030 ± 0.010 and for the Υ(9460), Γ = 0.042 ± 0.015. Thus the Γ is within the errors the same at the first disconnection containing a double hairpin as at the second which has the usually studied single hairpin.

Thus it is experimentally clear from the ψ and Υ systems that a double hairpin type disconnection in a Zweig diagram is strongly OZI suppressed. The likely reason the ππ decay is very strong in these channels is that it requires only two less hard gluons to bridge the disconnection. Possible arguments that disconnected Zweig diagrams involving new types of quarks, but which are not of a single hairpin type may not be OZI suppressed are obviously contradicted by these reactions. If one naively applies crossing to these reactions, one could naively convince oneself that they are related to Pomeron exchange and thus strong. This would lead to a wide ψ(3685) and a wide Υ(10,020) instead of the observed very narrow states. Thus the Zweig disconnected diagrams and the OZI rule are subtle mysteries which are often misunderstood.[6,15] Finally I have carefully avoided utilizing Zweig diagrams involving so-called Pomeron exchange since no one really knows what the Pomeron is, especially in these types of reactions.

But what if one introduces two-step processes or other complicated intermediate states or processes, other than hard multigluons to jump the disconnected part of the diagram. The author has discussed this[6,15] and shown that the OZI rule is peculiar in that you can defeat it by two-step processes or in QCD language changing the nature of the multigluon exchange needed in the one-step diagrams to a series of the ordinary OZI allowed gluon exchanges.

In other words, Zweig's diagrams are, based on all experimental observations, to be taken literally as one-step processes and the multigluon exchanges needed to connect disconnected parts of the diagrams are not to be tampered with. Why are these peculiarities observed? I cannot answer that. Neither can I answer why color exists, why confinement? Why quarks? etc. etc. etc. These are all concepts based on observation.

It is certainly consistent with all experimental observations in the ϕ, J/ψ and Υ systems that the OZI rule[25,15] works very well.* Therefore I assumed as an Ansatz that the OZI rule is universal for weakly coupled glue in Zweig disconnected diagrams involving creation or annihilation of new types of quarks, and of course the correctness of QCD as an Ansatz in drawing my conclusions. With these Ansatzen I will later conclude that we have discovered one or more glueballs. Without assuming QCD, there is no point in discussing glueballs. If you quarrel with assuming the universality of OZI, we will have to demote our conclusion of glueball discovery to discovery of very strong glueball candidates, and suggest you explain why the assumption of the OZI rule which has been consistently observed to work be replaced by complicated alternatives. <u>Remember, the name of the physics game is simplicity as long as it works!</u>

<u>The $\pi^- p \to \phi\phi n$ Experiment</u>

The experimental arrangement that BNL/CCNY used employing the new MPS II is shown in Fig. 3. The major changes from the MPS I experiments to MPS II experiments was to replace the spark chambers with drift chambers with ten times more data-gathering rate capability and to improve the (charged particle and γ) veto box around the liquid hydrogen target to obtain an even cleaner neutron signal.

Figure 4 is a scatter plot of the mass of one K^+K^- pair versus the mass of the second K^+K^- pair. Each event has two points on the plot due to the four possible combinations. The two ϕ bands stand out over the 4-kaon background. Where the two ϕ bands cross there is a black spot with peak intensity (corrected for resolution and double counting) greater than 1,000 times that of the

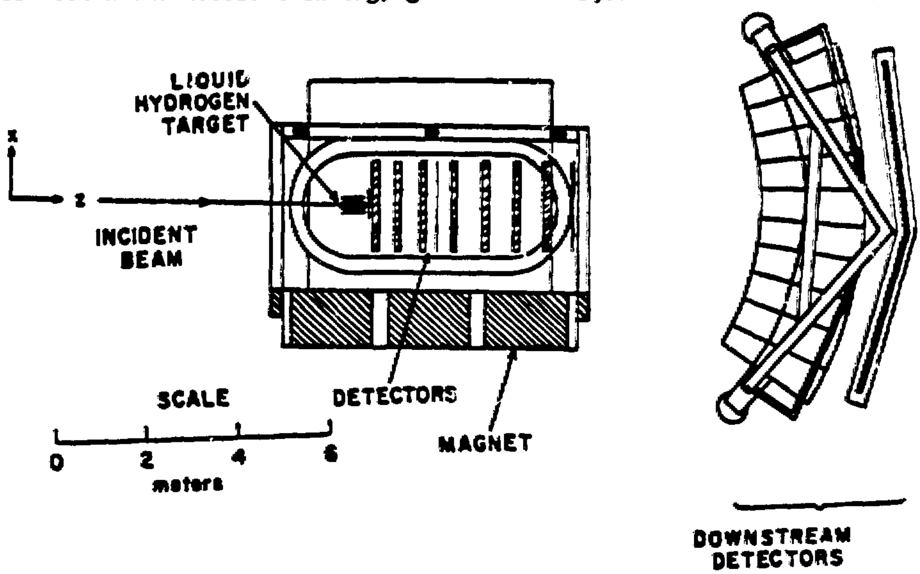

Figure 3: The MPS II and the experimental arrangement (see Ref. 3 for further details.

adjoining 4-kaon event intensity. The ϕ band intensity (corrected for resolution) is about a factor of 20 higher than the adjoining 4-kaon event intensity. Where the two ϕ bands cross, the $\phi\phi$ intensity (corrected for

---

* The fact that the OZI rule works well for the single ϕ, J/ψ and Υ is understandable if there are no glueballs with the right quantum numbers at their masses.

resolution) is ≈ 50 times greater than the $\phi(K^+K^-)$ intensity.* If the OZI suppression occurred, very little enhancement would be seen here. Thus we have a patent violation of the OZI suppression. This effect was noted by us in 1978.[4] The speaker has shown that if one uses the isobar model,[33] which is well known to work well and has no provision for OZI suppression, one can quantitatively explain[5,6,15] the scatter plot within a factor of 2. The new greater statistics data are consistent with the earlier experiment.

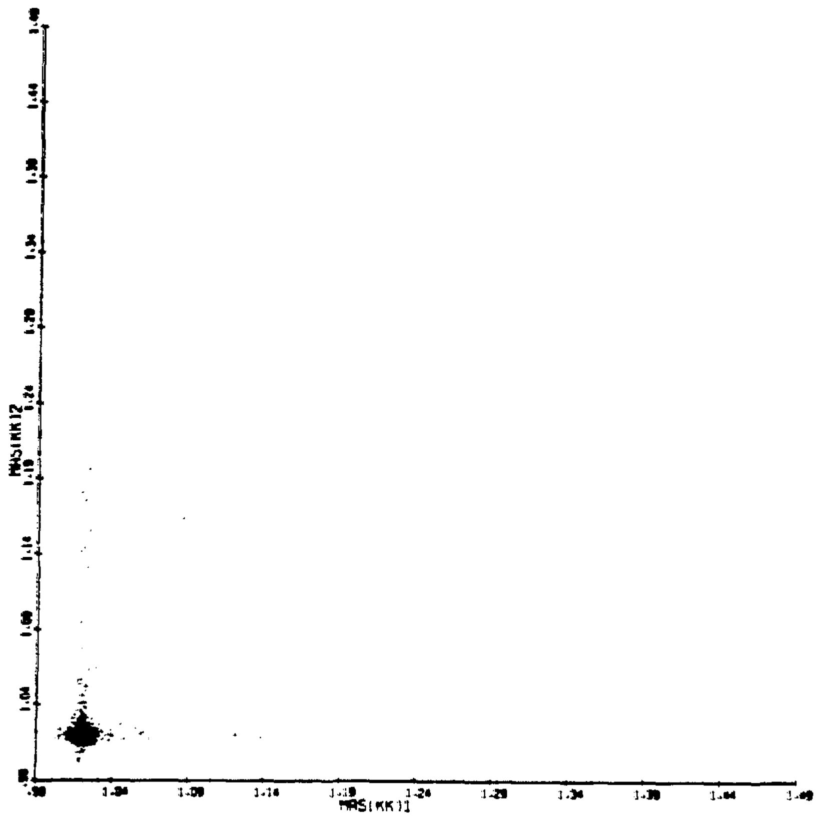

Figure 4: A scatter plot of K^+K^- effective mass. Two randomly chosen mass combinations are plotted for each event. Clear bands of $\phi(1020)$ are seen with an enormous enhancement (black spot) where they overlap (i.e. $\phi\phi$).

Independent evidence of the breakdown of the OZI suppression is given[34,35] by a study of the reaction $K^-p \to \phi\phi\Lambda$ or $\phi\phi\Sigma^0$. This OZI allowed reaction has a cross section only a factor ≈ 4 larger than the cross section for $\pi^-p \to \phi\phi n$ which

* When a huge signal occurs where none is supposed to, nature is usually trying to give you a message. Here I believe the message is "glueballs".

is OZI forbidden. We also have preliminary results on this reaction and obtain the same factor ≈ 4. One should divide the 4 by a factor of 2 since in the π^- case only n is allowed to accompany the $\phi\phi$, whereas in the K^- case, either a Λ or Σ^0 is accepted.

The OZI allowed and forbidden reactions have equal cross sections within a factor of 2. In contrast to this, the ratio[31]

$$\frac{\sigma(K^-p) \to \phi\Lambda}{\sigma(\pi^-p) \to \phi n} \approx 60$$

shows the typical OZI suppression. It has also been shown[35] recently that

$$\frac{\sigma(K^-p) \to \phi K^+K^-n}{\sigma(K^-p) \to \phi\phi n} \approx \frac{\sigma(\pi^-p) \to \phi K^+K^-n}{\sigma(\pi^-p) \to \phi\phi n} \approx 5$$

Since all states except $\pi^-p \to \phi\phi n$ are OZI allowed, this again shows the absence of OZI suppression.* Thus we have shown in a number of ways that the large OZI suppression ≈ 100, expected in single ϕ production is present, whereas that expected in $\phi\phi n$ production is broken down to within a factor of 2 of OZI allowed processes which is within the uncertainties of the comparisons. Thus we can clearly conclude that the expected OZI suppression is essentially asbsent in the $\pi^-p \to \phi\phi n$ OZI forbidden process. Figure 5 shows the mass spectrum of the other K^+K^- pair in an event when one K^+K^- pair falls in the ϕ mass band (1014.6 ± 14 MeV) and clearly indicates the huge $\phi\phi$ signal. Figure 6 shows a very clear neutron recoil from the $\phi\phi$ with an estimated contamination of non-neutron events in our data sample ≈ 3%. This should have a negligible effect on our analysis. In the mass region where the partial wave analysis was done, the ϕK^+K^- background was small (≈ 11%) and it was included in our analysis.

The histogram in Fig. 7 shows the detected $\phi\phi$ effective mass spectrum for 1203 $\pi^-p \to \phi\phi n$ with an estimated background of 130 events from ϕK^+K^- and ≈ 40 events of non-neutron recoil. The dashed line is the Monte Carlo determined acceptance of the apparatus for our partial wave analysis solution to be discussed later. However one should note that the result obtained for the acceptance is close to that one would obtain from phase space. Furthermore the results of the partial wave analysis are insensitive to considerable changes in the acceptance. The observed spectrum is consistent with that of Ref. 3 and other subsequent low statistics $\phi\phi$ experiments.[26] One should note that for

---

* $\sigma(K^-) \approx \sigma(\pi^-)$ for $\phi\phi$ production implies flavor independence (supporting glueballs). It should be noted that in general, strange quark production is enhanced by one to two orders of magnitude when a strange quark is contained in the initial system. This general effect has been greatly downgraded in this instance.

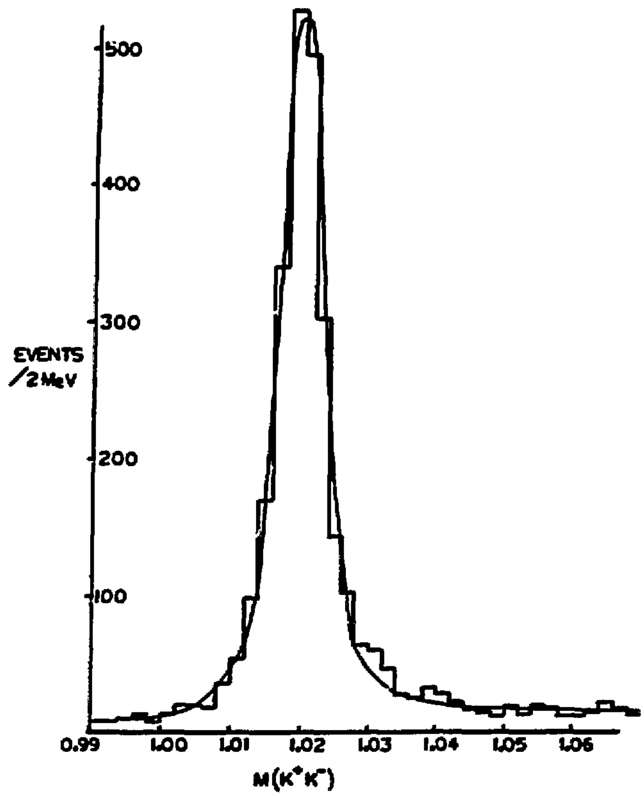

Figure 5: The effective mass of each K^+K^- pair for which the other pair was in the ϕ mass band.

$|t'| < 0.3$ GeV^2 the t' distribution is consistent with $e^{(9.4 \pm 0.7)t'}$. If one looks at the quark structure of Fig. 1c, one essentially has a pion exchange radiating several gluons (thought to represent a glueball) and thus one would expect a peripheral production mechanism, which is what we observe.

It should be noted that the $\phi\phi$ mass spectrum from $K^-p \rightarrow \phi\phi\Lambda/\Sigma$[34] is much broader and extends to much higher masses (see Fig. 8).

Partial Wave Analysis

The partial wave analysis (PWA) used six angles to specify all kinematic and other characteristics of the $\phi\phi$ system with each ϕ decaying into a K^+K^- pair.

Figure 9 shows the Gottfried-Jackson frame. The usual GJ angles, β (polar) and γ (azimuthal), were employed.

Figure 10 shows the rest frame of ϕ_1. In it we label the polar angle of the decay of the K_1^+ relative to the ϕ direction as θ_1, and the azimuthal angle of the decaying K_1^+ as α_1. There is a similar rest frame (not shown) for the second ϕ with corresponding polar angle for K_2^+ of θ_2 and azimuthal angle α_2. Since the

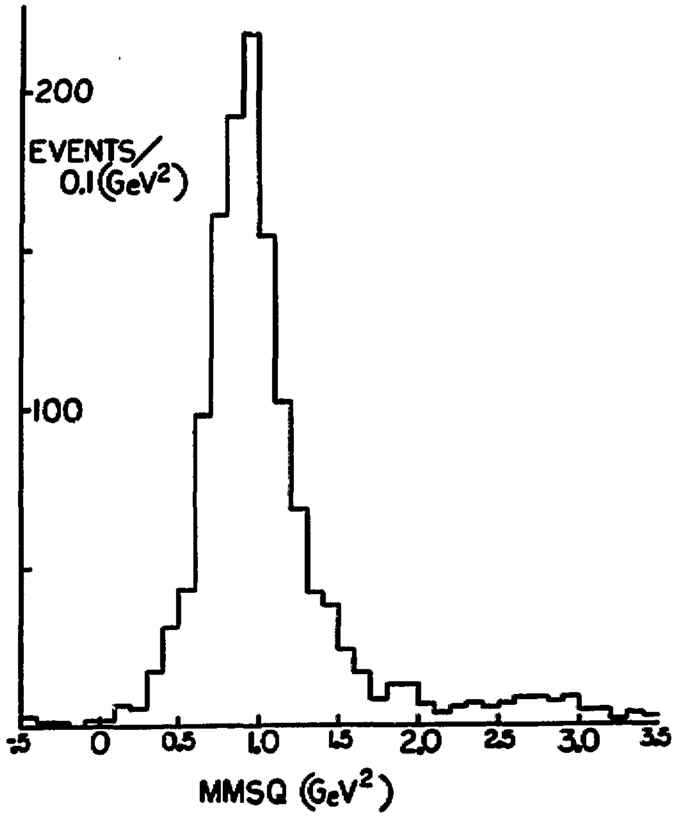

Figure 6: The missing mass squared for the neutral recoiling system from the $\phi\phi$.

azimuthal angles α are the same in either ϕ rest frame, α_2 is shown in the rest frame of α_1. These six angles and relevant combinations of them were used in the PWA.

The partial waves considered were all waves with J = 0,1,2,3,4; L = 0,1,2,3; S = 0,1,2; $-J \leq M \leq J$, P = ±, η = ±. J is the total angular momentum of the $\phi\phi$ system. L is the orbital angular momentum, M is J_z, P is the parity and η the exchange naturality of the wave. I = 0 and C = + for the $\phi\phi$ system. Bose statistics requires that L + S = even number.

The above criteria led to a group of 52 independent waves. The maximum likelihood method was used for the PWA. To determine the partial waves playing a major role in the $\phi\phi$ system, the events in the mass region 2.1 to 2.3 GeV were fitted with an incoherent background plus one additional partial wave of specific J^P, S, L, M and η, cycling through each of the 52 waves described above. The largest, and only significant contribution came from $J^{PC}SLM^{\eta} = 2^{++}200^{-}$. This wave was retained, and to search for other waves, each of the other 51 were added one at a time in turn. The only significant additional contribution came from

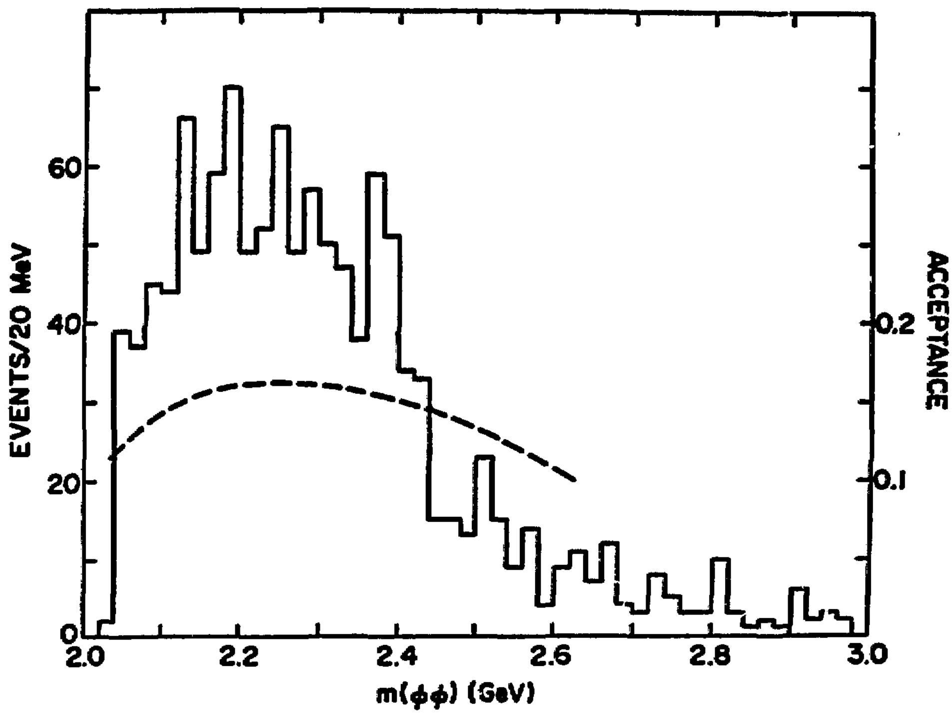

Figure 7: The observed φφ effective mass spectrum. The dashed line is the Monte Carlo calculated acceptance.

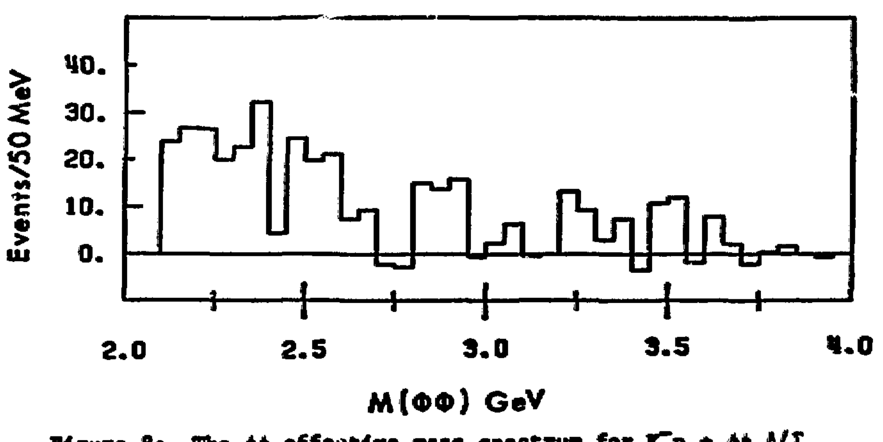

Figure 8: The φφ effective mass spectrum for $K^-p \to \phi\phi\ \Lambda/\Sigma$.

$J^P SLM^\eta = 2^+220^-$. These two waves were then retained and each of the remaining fifty were added one at a time in turn. No statistically significant contribution from any other wave was found. The φφ data were then divided up into five adjoining 100 MeV wide bins starting from threshold, so that we could

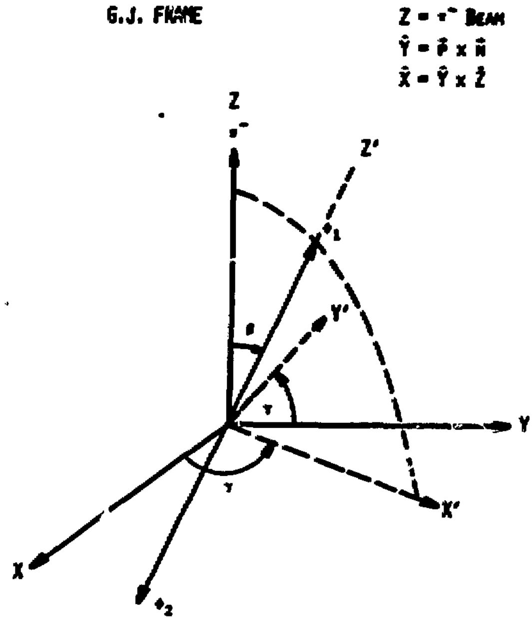

ϕ_1 AND ϕ_2 LIE IN (Z,X') PLANE

Figure 9: *The Gottfried-Jackson frame with polar angle β and azimuthal angle γ.*

explore the mass dependence of the partial wave structure. The bin size was chosen because about 200 events per bin are needed to obtain reliable solutions.

The background from ϕK^+K^- events (≈ 11%) was estimated from an examination of the regions adjacent to the $\phi\phi$ peak. There was no evidence of any angular structure, so this background was represented by a flat distribution in all angles. A maximum likelihood fit to the five bins using the two $J^P = 2^+$ waves described gave a very good fit with χ^2/D.F. ≈ 1 when the statistics and systematic errors were considered. To ensure that no other combination of two waves would give an equivalent fit, each possible combination of two waves, i.e. 52 x 51/2 = 1326, were tried in the central bin where the S and D waves found had a significant overlap. The closest one came to a fit was 5σ away from the original fit. These ≈ 5σ fits always had the S-wave originally found as one of the two waves. Hence the original two-wave fit is clearly selected.*

Therefore the mass independent solutions (i.e. no parameterization chosen) for the $J^PSLM^\eta = 2^+200^-$ S-wave and the 2^+220^- D-wave are shown in Fig. 11. The lower half of the figure shows the $|S|^2$ normalized to events as the open circle

* One might perhaps expect a background of the L = 0, $J^P = 0^+$ wave at threshold, but this wave contributes only 10 ± 5% of the events in the lowest mass bin. Furthermore, one should recall backgrounds do not break down OZI suppression.

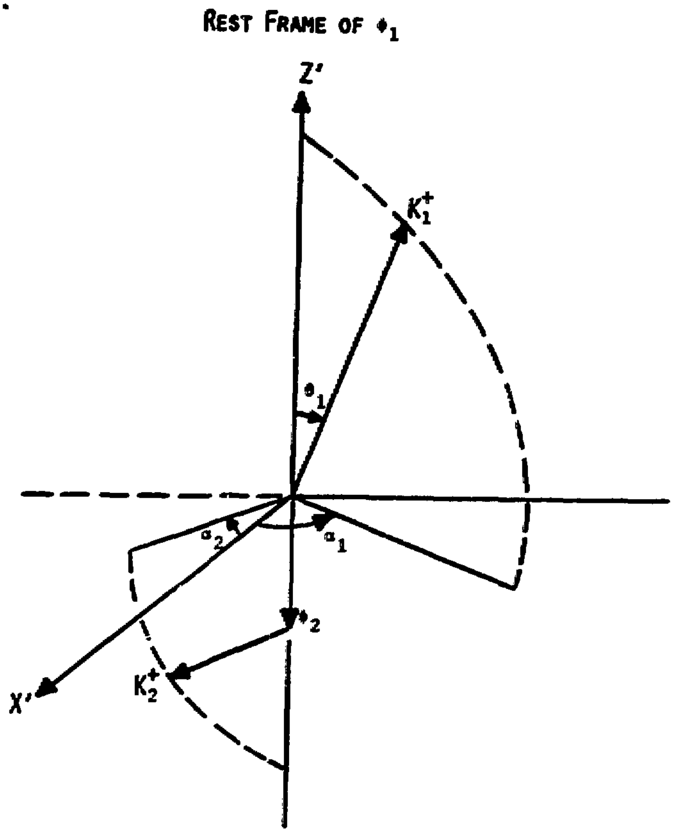

Figure 10: The ϕ rest frame with the polar angle θ_1 of the decay K_1^+ (relative to ϕ direction) and the azimuthal angle α_1 of the decay K_1^+.

points and the corresponding $|D|^2$ amplitudes squared are shown as the closed points. The x points in the upper part show the D-S phase difference. A natural parameterization for these data is one or two Breit-Wigners. A one Breit-Wigner fit was rejected by > 10σ, primarily because of the phase difference. A two Breit-Wigner fit on the other hand was very good with $\chi^2/D.F. = 1$. The solid lines show this fit. The quantum numbers and parameters of the two resonances to be discussed later, are shown in Table I.

It at first appears remarkable that we can demonstrate such selectivity (i.e. 2 waves selected out of 52). However this results from the fact that the $\phi\phi$ system is a very powerful analysis system for picking particular waves. If we look at Figs. 12a and 12b where angular variables for numerous allowed (i.e. L + S = even) pure waves up to $J^{PC} = 4^{++}$ are shown. We can notice from these figures that each wave has its own characteristic signature in the various variables shown. Our data shows a flat distribution in γ, all M = 0 waves which are shown have this feature. Therefore there is no need to plot γ. The primes (i.e. α_1' –

TABLE I

Quantum numbers and parameters of the Breit-Wigner resonance fit to the S- and D-wave amplitudes (and phase difference) of Fig. 11.

	$g_T(2160)$	$g_T(2320)$
$I^G J^{PC}$	0^+2^{++}	0^+2^{++}
Mass (GeV)	2.16 ± 0.05	2.32 ± 0.04
Γ_{tot}	0.31 ± 0.07	0.22 ± 0.07
Ratio of Partial Widths	$\Gamma_D/\Gamma_S = 0.02$	$\Gamma_S/\Gamma_D = 0.04$

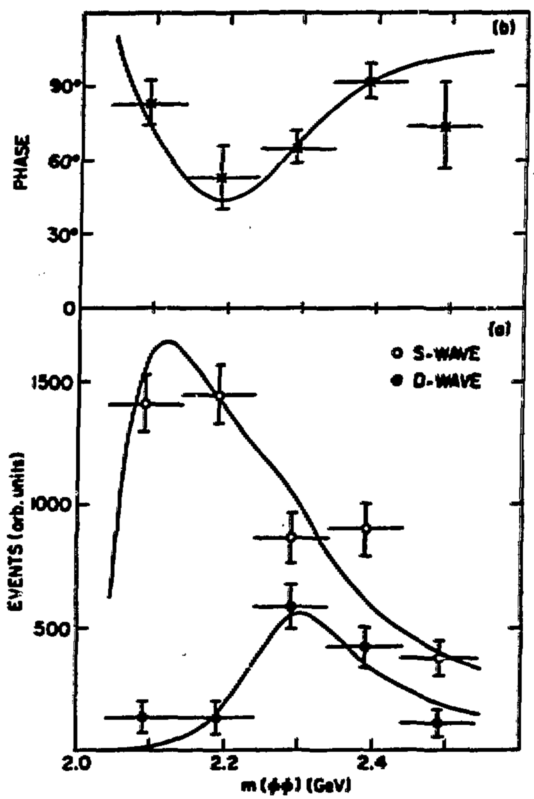

Figure 11: (a) The points show the intensity ($|S|^2$ and $|D|^2$) and for the best mass-independent two-wave fit described in the text. (b) The points show the D-S phase difference (mass-independent) for the best two-wave fit described in the text. The curves show the resultant best maximum likelihood fits for the parameterization of two interfering Breit-Wigner resonances.

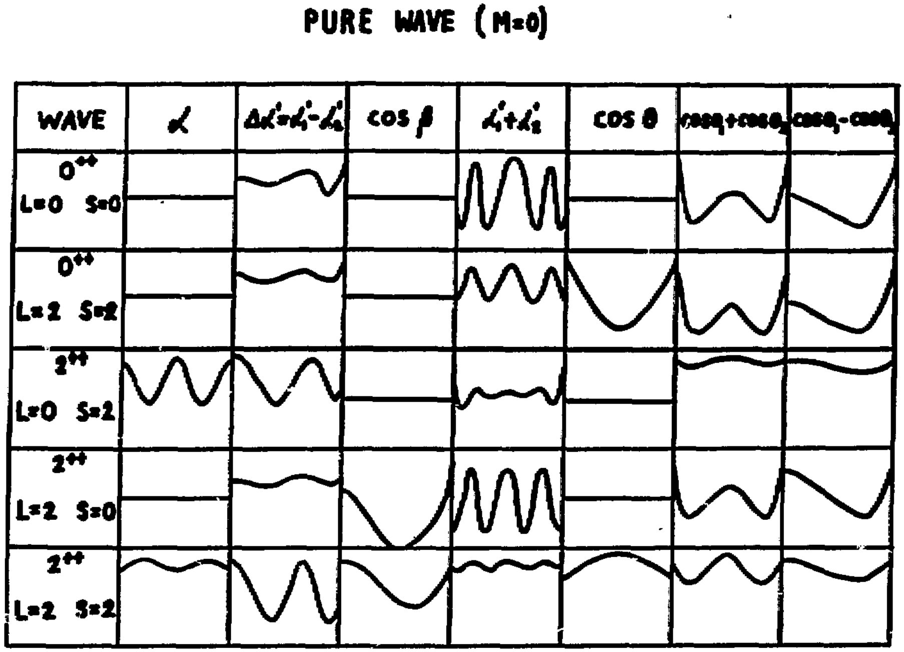

Figure 12a: Various pure waves from $J^{PC} = 0^{++}$ to $J^{PC} = 2^{++}$ with M = 0.

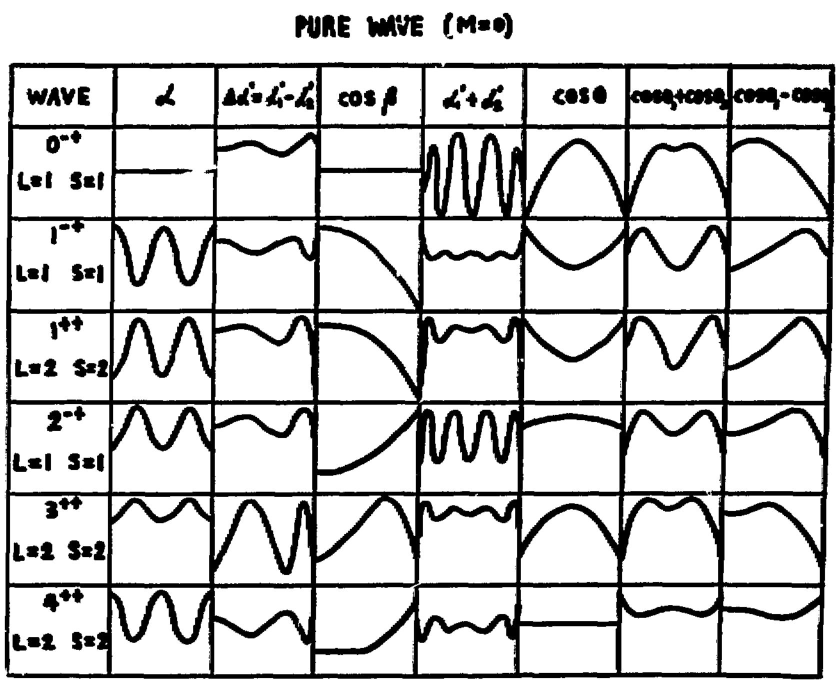

Figure 12b: Various pure waves from $J^{PC} = 0^{-+}$ to $J^{PC} = 4^{++}$ with M = 0.

α_2') indicate modifications to the variables for display and comparison purposes so as to equalize the phase space in each histogram bin (to be shown later). For example:

$$\Delta\alpha' = \frac{(\alpha_1 - \alpha_2)}{\pi} \frac{(1 - |\alpha_1 - \alpha_2|)}{4\pi} .$$

Due to the inherent symmetry, $\Delta\alpha' = \alpha_1' - \alpha_2'$, and $\cos\theta_1' - \cos\theta_2'$ have been folded, the data for α_1 and α_2 added, and the data for $\cos\theta_1$ and $\cos\theta_2$ added. The very characteristic signature for particular pure waves in these angular variables give us great selectivity. Notice that the two $J^P = 2^+$ (S and D) waves found in the PWA (the third and the fifth from the top in Fig. 12a) have similar very characteristic large structure in $\alpha_1' - \alpha_2'$ and the S-wave has a characteristic structure in α whereas the D-wave does not. Thus $\alpha_1' - \alpha_2'$ and α are the most important variables in selecting the $J^{PC} = 2^{++}$ waves we found in our partial wave analysis.

A detailed comparison (in 3 mass bins) of the data and the Monte Carlo generated prediction for our fit from the partial wave analysis is shown. The Monte Carlo results are acceptance-corrected and are based on over 14,000 events, more than an order of magnitude more statistics than the data (for which the actual number of events are shown). Thus the statistical fluctuations in the Monte Carlo results will be small compared to those in the data. We determined that the angular variables and correlations were not sensitive to the acceptance except in the case of the G.J. angle β.

A comparison of the data and the Monte Carlo for γ (the G.J. azimuthal angle) are compared in Fig. 13a. The agreement is very good.

The data and Monte Carlo for $\cos\beta$, where β is the G.J. polar angle are compared in Fig. 13b. Even though $\cos\beta$ is sensitive to the acceptance, we obtain a quite reasonable agreement.

Figure 14 shows the data and Monte Carlo predictions of the fit for α and $\Delta\alpha' = \alpha_1' - \alpha_2'$. The agreement between the data and the Monte Carlo prediction based on the fit for $\Delta\alpha'$ is most impressive since there are large factors $\gtrsim 3$ between peaks and valleys.

The agreement is also quite good for α. The first bin shows large structure, characteristic of the S-wave. The next bin shown is where the D-wave is very important and shows very little structure in α, which is a feature of the D-wave. The agreement is good. The next bin shows the structure returning as the D-wave drops down and again indicates agreement.

Figure 15 shows the comparison of the data with the Monte Carlo for $\alpha_1' + \alpha_2'$ and $\cos\theta$. There is no sizeable structure in these variables. The agreement is generally good.

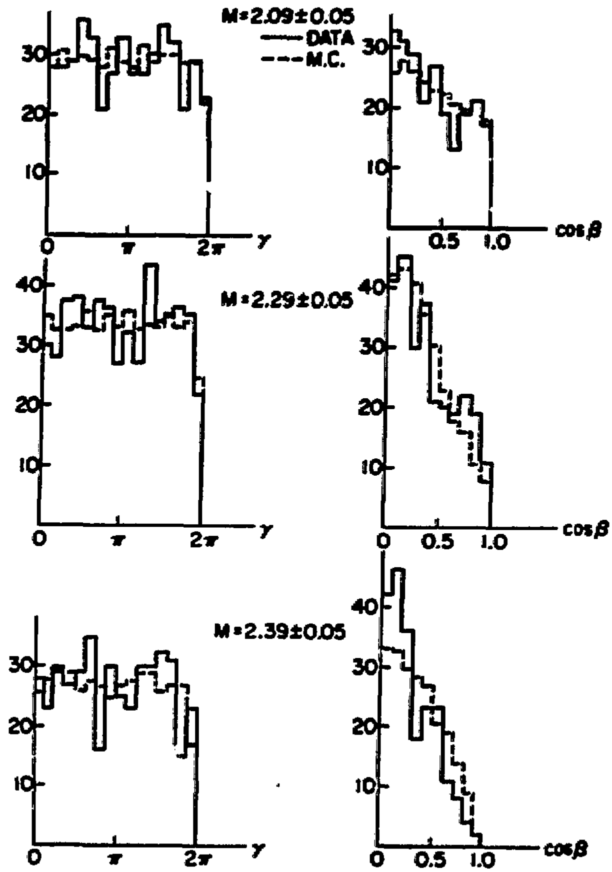

Figure 13: (a) Comparison of the data and the acceptance-corrected Monte Carlo for the fit in G.J. azimuthal angle γ.

(b) Comparison of the data and the acceptance-corrected Monte Carlo for the fit in G.J. polar angle function cosβ.

Figure 16 shows the comparison of the data with the Monte Carlo for $\cos\theta_1' - \cos\theta_2'$ and $\cos\theta_1' + \cos\theta_2'$. The agreement is good and there is no sizeable structure in these variables.

We have made ten characteristic angular correlations for six independent variables and found good agreement - striking at times in Δα' and α for example. The data and Monte Carlo agree in all mass bins in all variables.

In Fig. 17 where the solid line is the fit prediction, the agreement with the ϕϕ mass spectrum is also good. However, in the ϕϕ system, its myriad and characteristic angular distributions and angular correlations are much more important tests of the significance of the fit, than the mass spectrum. Thus we

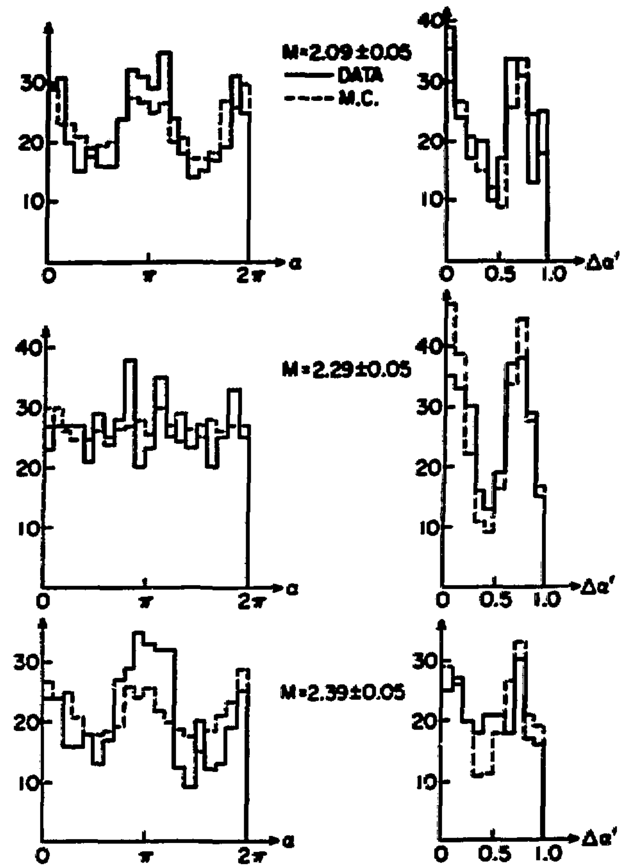

Figure 14: (a) Comparison of the data and the acceptance-corrected Monte Carlo for the azimuthal angle α of the decay K^+ in the ϕ rest frame.
(b) Comparison of $\Delta\alpha' = \alpha_1' - \alpha_2'$ with the acceptance-corrected Monte Carlo for the fit.

can feel quite confident that our two Breit-Wigner fits are in excellent agreement with the data.

All the quantum numbers, the mass, full width, and partial width ratios for these two Breit-Wigner resonances are given in Table I. They are at the very least strong glueball candidates due to the breakdown of the OZI suppression, and the striking selectivity of 2 out of 52 possible waves selected.

If one takes as input Anzatsen: 1) the correctness of QCD; 2) the universality of the OZI rule for weakly coupled glue in a disconnected Zweig diagram, due to introduction of a new type of $q\bar{q}$ pairs, this leads to OZI suppresion due to a weakly coupled hard multigluon exchange. As I have pointed out previously, a glueball in which the gluons resonate would lead to effectively strongly-coupled glue, and break down the OZI suppression.

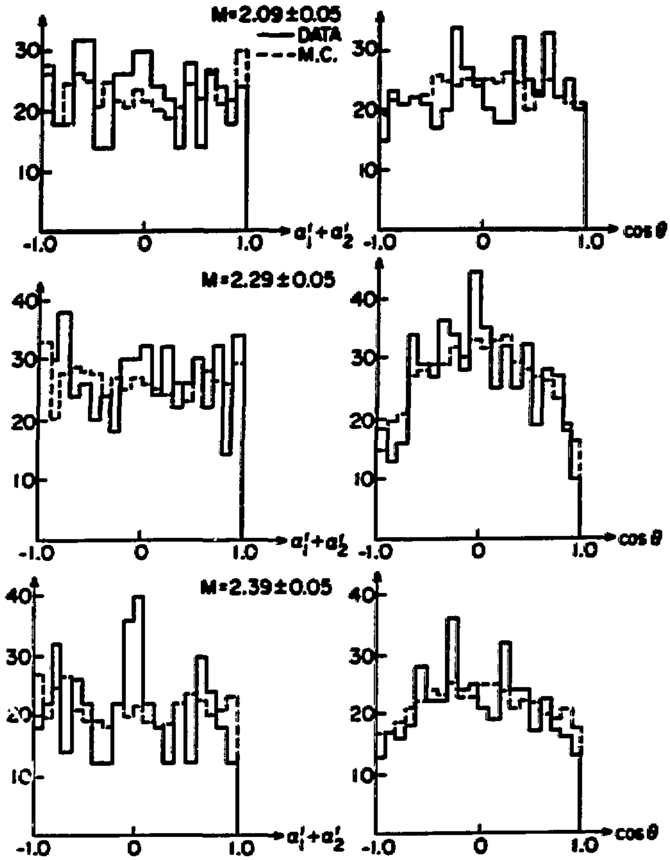

Figure 15: (a) Comparison of the data and the acceptance-corrected Monte Carlo for $\alpha_1' + \alpha_2'$.
(b) Comparison of the data and the acceptance-corrected Monte Carlo fr. cosθ.

This leaves me as the only explanation of the OZI suppression breakdown and the observed selectivity, the presence of one or two primary glueballs in the mass region with these quantum numbers. Impure $q\bar{q}$ intermediate states, 4-quark states, etc. are ruled out by the above Ansatzen (Ansatz 2).

I say one or two primary glueballs because one primary glueball could break down the OZI suppression and possibly mix with a nearby quark state with the same quantum numbers yielding two states very rich in resonating glue. Of course, both states could come from different primary glueballs* since we expect that there is a glueball spectrum of states - not just a single glueball.

* They might also eventually dress themselves to some degree with $q\bar{q}$ pairs.

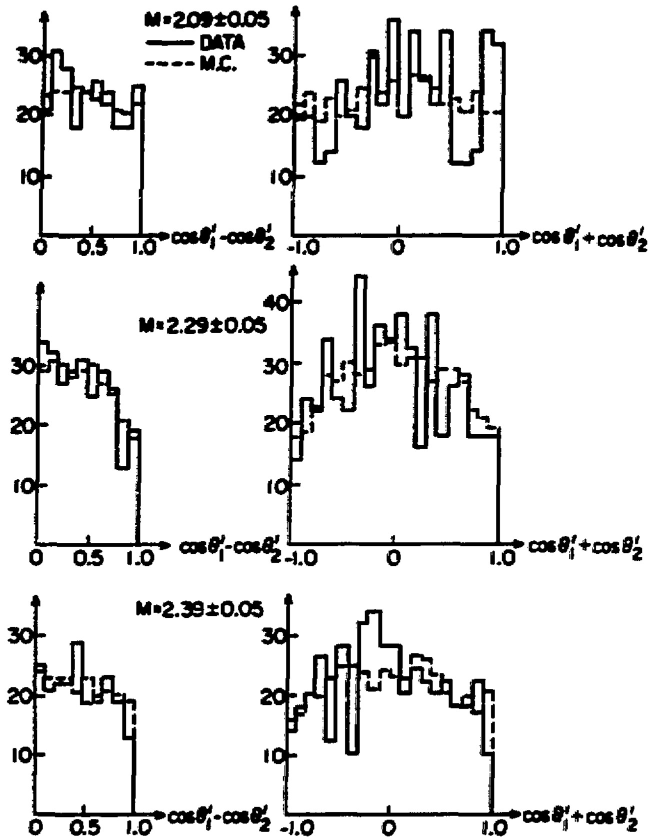

Figure 16: (a) Comparison of the data and the acceptance-corrected Monte Carlo for $\cos\theta_1' - \cos\theta_2'$.
(b) Comparison of the data and the acceptance-corrected Monte Carlo for $\cos\theta_1' + \cos\theta_2'$.

In a number of papers it was concluded that the width of a glueball should be narrower than hadronic resonances typically by a factor ≈ $\sqrt{\text{OZI suppression}}$ factor. These considerations were based on treating the quark-glue, glue-glue coupling as weak, and clearly do not apply if the glue-glue coupling becomes strong enough to form a resonance, in which case we are generally dealing with a very strongly interacting multigluon resonance. The glue-glue coupling is effectively stronger than the quark-glue coupling, and hadronization is thought to occur at large distances after splittings and involves considerable numbers of softer gluons. Therefore glueballs in general should be as wide, or wider than, typical hadronic resonances in the mass region (see Table II).

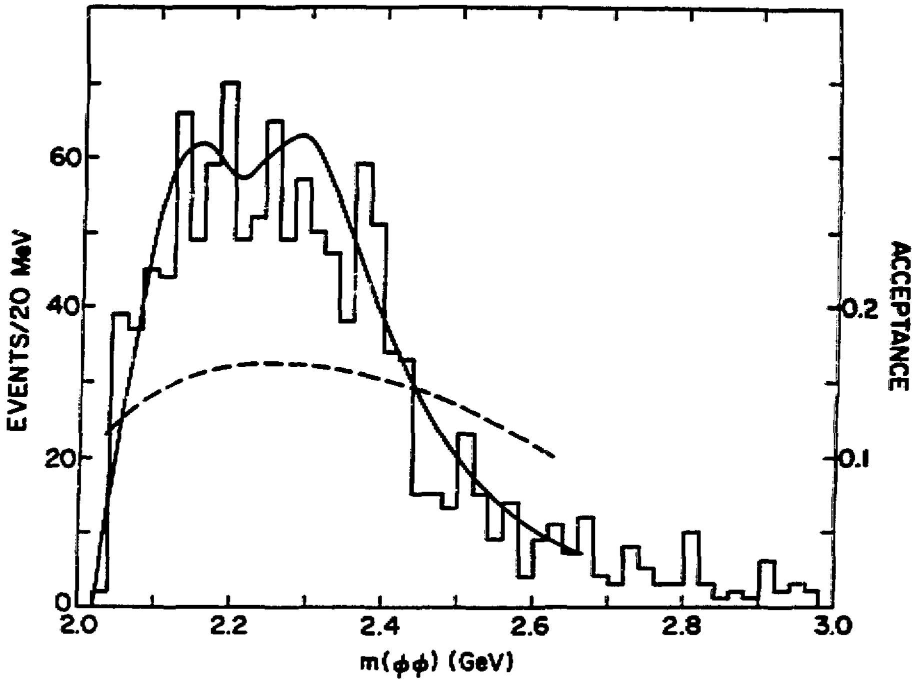

Figure 17: The observed φφ mass spectrum compared to the predicted (solid line curve) mass spectrum from the acceptance-corrected fit. The dashed line is the acceptance.

However, Sid Meshkov's "oddballs" (exotic J^{PC})[11,13,24] may be narrow since we have no knowledge of how exotic states couple. We estimate that we need at least an order of magnitude more data to search for "oddballs", and plan to accumulate this additional data in the next 1-2 years.

Table II lists some typical resonance widths from the particle data group tables and widths for other glueball candidates. We see that Γ = (200-300) ± 100 MeV are reasonable values for glueballs.

Phenomenological Predictions for Glueballs

In constituent glueball models[13] the gluon is considered to have an effective mass m_g = 0.75 GeV,[36] due to confinement. Thus we might be in the three-gluon sector. Due to the self-coupling between the gluons and their splittings, a gauge invariant description with a definite number of gluons is not possible. Nevertheless it is physically appealing and reasonable to expect in constituent gluon models that the lowest lying ground state would be mostly

TABLE II

Resonance Widths for Some Hadronic Resonances from the Particle Data Group Table[32]

State	$I^G(J^P)C_n$	Full Width Γ in MeV
g(1690)	$1^+(3^-)-$	200 ± 20
ρ'(1600)	$1^+(1^-)-$	300 ± 100
f(1270)	$0^+(2^+)+$	179 ± 20
Resonance Widths for Other Glueball Candidates[9,10,16]		
SLAC iota(1440)	$(0^-)+$	55^{+20}_{-30}
θ(1640)	$(2^+)+$	220^{+100}_{-70}
BNL/CCNY g_s(1240)	$0^+(0^{++})$	140 ± 10

composed of 2 gluons and have a mass ≈ 2 x 0.75 GeV ≈ 1.5 GeV. One would expect another ground state in the 3g sector mostly composed of 3 gluons with a mass ≈ 3 x 0.75 GeV ≈ 2.25 GeV.

MIT bag calculations of glueballs assume massless gluons and obtain predictions for quantum numbers and masses of various states.[37,38] The masses do not fit some present glueball candidates. Hyperfine energy shifts that depend on α_s have been put into the bag calculations to allow such fits.[39] Adapting these methods, we have derived m_g for two-gluon states as a function of α. The SLAC iota (1440) and θ(1640) glueball candidates, and the BNL/CCNY g_s(1240) glueball candidate, were used as inputs to derive the results shown in Fig. 18. We can obtain a $J^{PC} = 2^{++}$ g_T(2160) at about the right mass as an excited state in the 2g sector.* A recent calculation[38] based on the MIT bag has shown that a low-lying $(TM)^2$ glueball has an estimated mass in the region ≈ 2.4 GeV.

The massless assumption for gluons in the bag does not allow $J^{PC} = 2^{++}$ for low-lying 3-gluon states, in contrast to the constituent gluon model which allows all J^{PC} for 3g states and all J^{PC} (i.e., C = +) for 2g states.

So far, lattice calculations[40] have concentrated mainly on the glueball ground state getting $J^{PC} = 0^{++}$, M ≈ 0.8 – 1.0 GeV. Recently they have begun to

* However, one should be aware that perturbative treatments are not justifiable at high values of α_s.

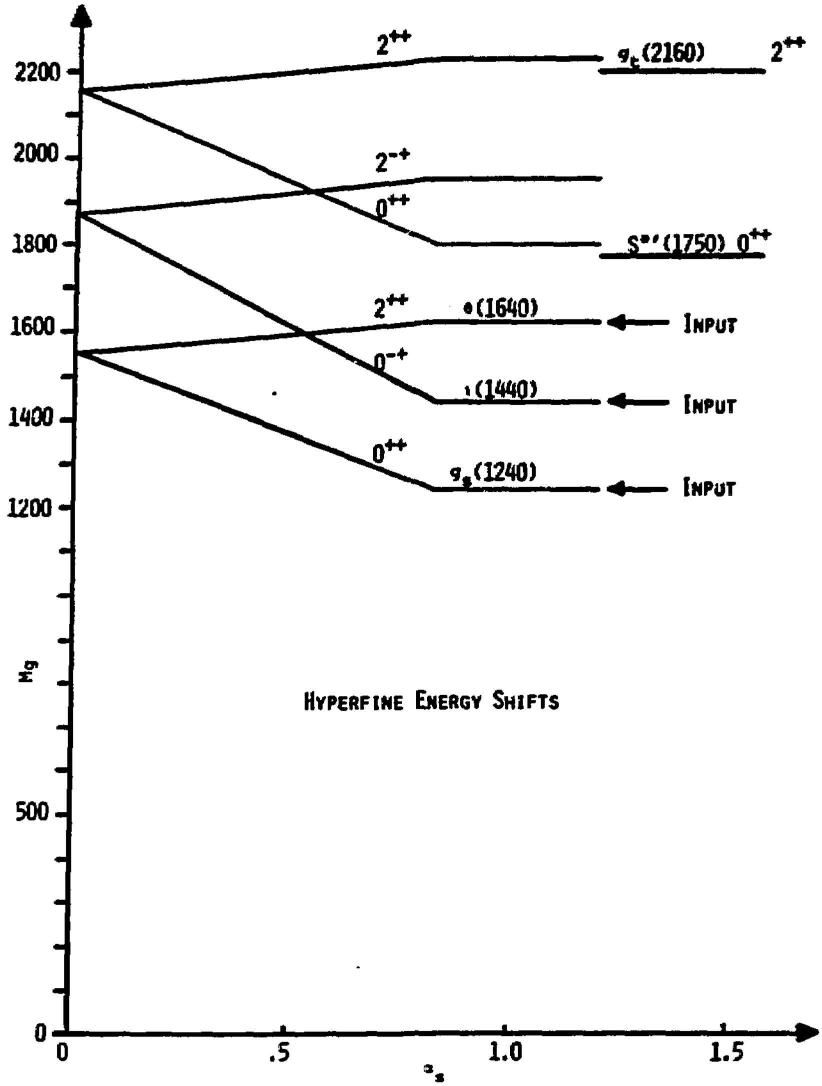

Figure 18: The predicted mass and quantum numbers of the 2g glueballs from adapting the methods of Ref. 39. The iota (1440), θ(1640) and g_s (1240) were used as input to determine the overall mass level, the spacing between the levels, and α_s (till break in lines).

attack higher spin states.[41,42] The work is still preliminary, but indications are that higher spin states could well show up in our mass region. Thus, in summary, one finds that the phenomenological models are generally compatible with our results, except for the MIT bag calculations if we are in the 3g sector.

Conclusions for the $\pi^- p \to \phi\phi n$ Channel Experiment

If you assume as input Ansatzen: 1) QCD is correct, and 2) The OZI Rule is universal for weakly coupled glue in disconnected Zweig diagrams, due to the creation or annihilation of new types of quarks, then we have discovered one or two primary glueballs with $I^G = 0^+$, $J^{PC} = 2^{++}$ which lead to the observed states:

$g_T(2160)$ $\quad$ $M = 2160 \pm 50$ MeV, $\Gamma = 310 \pm 70$ MeV

$g_T(2320)$ $\quad$ $M = 2320 \pm 40$ MeV, $\Gamma = 220 \pm 70$ MeV.

References:

1. C.N. Yang and R.L. Mills, Phys. Rev. 96, 191 (1954).
2. a) Fritzch and Minkowski, Nuovo Cimento 30A, 393 (1975).
   b) R.P. Freund and Y. Nambu, Phys. Rev. Lett. 34, 1645 (1975).
   c) R. Jaffe and K. Johnson, Phys. Lett. 60B, 201 (1976).
   d) Kogut, Sinclair and Susskind, Nucl. Phys. B114, 199 (1975).
   e) D. Robson, Ncl. Phys. B130, 328 (1977).
   f) J. Bjorken, SLAC Pub. 2372.
3. A. Etkin, K.J. Foley, J.H. Goldman, W.A. Love, T.W. Morris, S. Ozaki, E.D. Platner, A.C. Saulys, C.D. Wheeler, E.H. Willen, S.J. Lindenbaum, M.A. Kramer, U. Mallik, Phys. Rev. Lett. 40, 422 (1978).
4. A. Etkin, K.J. Foley, J.H. Goldman, W.A. Love, T.W. Morris, S. Ozaki, E.D. Platner, A.C. Saulys, C.D. Wheeler, E.H. Willen, S.J. Lindenbaum, M.A. Krame and U. Mallik, Phys. Rev. Lett. 41, 784 (1978).
5. S.J. Lindenbaum, Hadronic Physics of $q\bar{q}$ Light Quark Mesons, Quark Molecules and Glueballs. Proc. of the XVIII Course of the International School of Subnuclear Physics, July 31-August 11, 1980, Erice, Trapani, Italy, Subnuclear Series, Vol. 18, "High Energy Limit", Ed. A. Zichichi, pp. 509-562.
6. S.J. Lindenbaum, Il Nuovo Cimento, 65A, 222 (1981).
7. P. Fishbane, Glueballs, A Little Review. Talk presented at the 1981 ORBIS Scientiae, Ft. Lauderdale, Florida (to be published).
8. D.L. Scharre, Glueballs, A Status Report. ORBIS Scientiae 1982, Miami, Florida (to be published), and SLAC Report 2880 (1982).
9. Edwards et al., Phys. Rev. Lett. 48, 458 (1982); 49, 259 (1982).
   M. Chanowitz, Phys. Rev. Lett. 46, 981 (1981).
11. C.E. Carlson, J. Coyne, P.M. Fishbane, F. Gross and S. Meshkov, Phys. Lett. 98B, 110 (1981).
12. J.F. Donoghue, K. Johnson and B. Li, Phys. Lett. 99B, 416 (1981).
13. a) C. Carlson, J. Coyne, P. Fishbane, F. Gross, S. Meshkov, Phys. Rev. D 23, 2765 (1981).
    b) J. Coyne, P. Fishbane and S. Meshkov, Phys. Lett. 91B, 259 (1980); C. Carlson, J.Coyne, P. Fishbane, F. Gross and S. Meshkov, Phys. Lett. 99B, 353 (1981).
14. a) S.J. Lindenbaum, Proc. Sixteenth Rencontre De Moriond, "New Flavours and Hadron Spectroscopy, Vol. II, pg. 187, Ed., J. Tran Thanh Van (Editions Frontieres, France, 1981); H.J. Schnitzer, ibid. pg. 648; K.R. Schubert, ibid. pg. 635.
    b) S.J. Lindenbaum, "Evidence for Glueballs", Proc. 1981 EPS Int. Conf. on High Energy Physics, July 9-15, 1981 (Calouste Gubenkian Foundation, Av. Berne, Lisbon, Portugal) (to be published).
    c) F.E. Close, "Glueballs, Hemaphrodites and QCD Problems for Baryon Spectroscopy", ibid.
15. a) S.J. Lindenbaum, Evidence for Explicit Glueballs From the Reaction $\pi^- p \to \phi\phi n$. Lecture presented at the 20th Course: Gauge Interactions; Theory and Experiment, International School of Subnuclear Physics, Erice, August 3-14, 1982 (to be published in proceedings); Also BNL 32096, October 1982.

References (continued):

15. b) S.J. Lindenbaum, Evidence for Glueballs. Proc. 1982 APS Meeting of the Division of Particles and Fields, University of Maryland, College Park, Maryland, October 28-30, 1982 (to be published). BNL 32188.
16. A. Etkin, K.J. Foley, R.S. Longacre, W.A. Love, T.W. Morris, S. Ozaki, E.D. Platner, V.A. Polychronakos, A.C. Saulys, Y. Teramoto, C.D. Wheeler, E.H. Willen, K.W. Lai, S.J. Lindenbaum, M.A. Kramer, U. Mallik, W.A. Mann, R. Merenyi, J. Marraffino, C.E. Roos, M.S. Webster, Phys. Rev. D 25, 2446 (1982).
17. C.E. Carlson, T.H. Hansson and C. Peterson, "Meson, Baryon and Glueball Masses in the MIT Bag Model", CTP #1020, August 1982 (submitted to Phys. Rev. D).
18. P.M. Fishbane, G. Karl, and S. Meshkov, "The iota(1440) and θ(1640) in a Mixing Model," UCLA82/TEP/18, October 1982.
19. a) J.F. Donoghue, Experimental Meson Spectroscopy - 1980, Sixth Int. Conf., Brookhaven National Laboratory, April 25-26, 1980, Eds. S.U. Chung and S.J. Lindenbaum, AIP Conf. Prof. #67, Particles and fields Subseries #21, pg. 1040.
    b) G. Bhanot, Phys. Lett. 101B, 95 (1981).
    c) G. Bhanot and C. Rebbi, Nucl. Phys. B180, 469 (1981).
    d) H. Hamber and G. Parisi, Phys. Rev. Lett. 47, 1792 (1981).
20. a) E. Bloom, 21st Int. Conf. on High Energy Physics, Paris, France, 26-31 July 1982, Journal de Physique 43, p. C3-407.
    b) J. Donoghue, ibid., p. C3-89.
21. W. Lockman, these proceedings.
22. S. Pinski, these proceedings.
23. J. Donoghue, these proceedings.
24. S. Meshkov, these proceedings.
25. a) S. Okubo, Phys. Lett. 5, 165 (1963); G. Zweig, CERN Report TH401 and 412 (1964); J. Iizuba, Prog. Theor. Phys. Suppl. 37-38, 21 (1966); J. Iizuba, K. Okuda and O. Shito, Prog. Theor. Phys. 35, 1061 (1966); S. Okubo, "A Survey of the Quark Line Rule," Univ. Rochester Report UR 641 (1977).
    b) S. Okubo, Phys. Rev. D 16, 2336 (1977).
    c) T. Applequist, K. Kane and M. Barnett, Ann. Rev. Nucl. Sci. 28, 387 (1978).
    d) I.J. Muzinish and F.E. Paige, Phys. Rev. D 21, 1151 (1980).
    e) S.J. Lindenbaum, "Quark Line Diagrams, Rules, and Some Recent Data," BNL 50812 (December 1977)
26. T.A. Armstrong et al., Nucl. Phys. B 196, 176 (1982); C. Daum et al., Phys. Letts. 104B, 246 (1981). The narrow enhancement in ϕ pairs produced from Be as reported in the latter paper is not confirmed by higher statistics result reported in contributed papers by C. Baum et al., and by B.R. French et al. at the 21st Int. Conf. on High Energy Physics, Paris, France, 26-31 July 1982. D. Green presented some very preliminary ϕϕ inclusive results produce by 400 GeV p-p collisions at this (Rencontre de Moriond) conference.
27. S. Eiseman, A. Etkin, K.J. Foley, R.S. Longacre, W.A. Love, T.W. Morris, S. Ozaki, E.D. Platner, V.A. Polychronakos, A.C. Saulys, C.D. Wheeler, S.J. Lindenbaum, M.A. Kramer, Y. Teramoto. "The MPS II Drift Chamber System", paper submitted to the IEEE 1982 Nuclear Science Symposium, October 20-22, 1982, Washington D.C. (IEEE Trans. on Nucl. Sci., in press).
28. H. Fritzch and M. Gell-Mann, XVI Int. Conf. on High Energy Physics, Chicago-Batavia, 1972, Vol. 2, p. 135; H. Fritzch, M. Gell-Mann and H. Leutwyler, Phys. Lett. 47B, 365 (1973); S. Weinberg, Phys. Rev. Lett. 31, 49 (1973); S. Weinberg, Phys. Rev. D8, 4482 (1973); D.J. Gross and F. Wilczek, ibid, 3633 (1973).
29. a) S.J. Lindenbaum, C. Chan, A. Etkin, K.J. Foley, M.A. Kramer, R.S. Longacre, W.A. Love, T.W. Morris, E.D. Platner, V.A. Polychronakos, A.C. Saulys, Y. Teramoto, C.D. Wheeler, "A New Higher Statistics Study of $\pi^- p \rightarrow \phi\phi n$ and Evidence for Glueballs." 21st Int. Conf. on High Energy Physics, Paris, France, 26-31 July 1982, Journal de Physique 43, p. C3-87.

References (continued):

29. b) A. Etkin, K.J. Foley, R.S. Longacre, W.A. Love, T.W. Morris, E.D. Platner V.A. Polychronakos, A.C. Saulys, C.D. Wheeler, C.S. Chan, M.A. Kramer, Y. Teramoto. "The Reaction $\pi^- p \rightarrow \phi\phi n$ and Evidence for Glueballs." Phys. Rev. Letts. 49, 1620–1623 (1982).
30. D. Cohen et al., Phys. Rev. Lett. 38, 269 (1977).
31. D.S. Ayres et al., Phys. Rev. Lett. 32, 1463 (1974).
32. Particle Data Group Tables, Phys. Letts. 111B, 12 (1982).
33. S.J. Lindenbaum and R.M. Sternheimer, Phys. Rev. 105, 1874 (1957); 106, 1107 (1957); 109, 1723 (1958); 123, 331 (1961).
34. T. Armstrong et al., CERN EP/82-103 (1982).
35. M. Baubillier et al., "Study of the Reaction $K^- p \rightarrow \phi\phi\Lambda$ at 8.25 GeV/c," paper submitted to Phys. Lett. B (September 1982).
36. G. Parisi and R. Petronzio, Phys. Lett. 94B, 51 (1980).
37. J.F. Donoghue, K. Johnson and Bing An Li, CTP #891 UN HEP-139, October 1980.
38. C.E. Carlson, T.H. Hansson and C. Peterson, "Meson, Baryon, and Glueball Masses in the MIT Bag Model," Paper submitted to Phys. Rev. D. (1982).
39. T. Barnes, F.E. Close and S. Monogham, Phys. Lett. 110B, 159 (1982).
40. C. Rebbi, 21st Int. Conf. on High Energy Physics, Paris, France, 26-31 July 1982, Journal de Physique 43, p. C3-723.
41. B. Berg, "Calculations in 4d Lattice Gauge Theories".
42. Petronzio, these proceedings.